A relationship between joint roughness and joint shear strength

Relation entre la rugosité des fissures et la résistance au cisaillement

Eine Relation zwischen Fugenrauheit und Fugenscherfestigkeit

N.R. BARTON, Norges Geotekniske Institutt, Oslo - Norvège

SUMMARY.

Tension fractures generated in different strengths of a weak, brittle model material are taken to represent joint surfaces of different dimensions. Direct shear tests performed on these surfaces suggest that, as far as peak shear strength is concerned, no appreciable strength-scale effect exists.

Analysis of the experimental results for a large number of shear tests on model joints reveals that a linear relationship exists between the peak dilation angle and the peak stress ratio. It is also found that a simple relationship exists between the peak dilation angle and the ratio of the normal stress to the compressive strength.

A simple method is developed for statistically analysing the roughness profiles recorded for joints of varying degrees of roughness. This involves the computation of inclination angles for asperities of different base lengths. It is found that these quantities are analogous to the change of peak dilation angles for different normal stresses.

The practical application of this shearing analogy to slope stability problems is summarised, and a typical example enumerated. Photogrammetric recording of the roughness of joints exposed on rock faces, and a statistical analysis of the data, provides an estimate of the peak shear strength for any range of normal stress.

RÉSUMÉ.

Des fissures de tension différentes provoquées dans un matériau d'essai faible et fragile sont choisies pour représenter des surfaces de fissures de différentes dimensions. Des essais directs de cisaillement effectués sur ces surfaces font penser, en ce qui concerne la résistance limite au cisaillement, qu'il n'existe aucun effet résistance-échelle de valeur notable.

L'analyse des résultats expérimentaux obtenus à l'aide d'un grand nombre d'essais de cisaillement sur des fissures sous forme de modèles, montre qu'il

existe une relation linéaire entre l'angle maximum de dilatation et le rapport des contraintes maximum. On a révélé également l'existance d'une relation simple entre l'angle maximum de dilatation et le rapport tension normale / force de compression.

Une méthode simple est développée destinée à servir dans l'analyse statistique des profils de rugosité enregistrés pour les différents degrés de rugosité. A ce sujet, il faut calculer les angles de pente des aspérités de longueurs de base différentes. On a constaté que ces valeurs sont analogues à la variation des angles maximum de dilatation pour différentes tensions normales.

Compte est rendu sommairement de l'application pratique, aux problèmes posés par la stabilité des talus, de cette analogie de cisaillement, et un exemple typique est étudié. L'enregistrement photogrammétrique de la rugosité de fissures exposées (fissures de surface de rochers), et une analyse statistique des données, permettent d'obtenir une appréciation de la résistance limite au cisaillement pour toutes tensions normales.

ZUSAMMENFASSUNG.

Zugrisse, die verschiedentlich in einem schlechten und spröden Material hervorgerufen werden, wurden als Fugenflächen von verschiedenen Grössen betrachtet. Direkte Scherversuche an diesen Flächen zeigten, dass, soweit der Grösstwert der Scherfestigkeit betroffen ist, keine unterschiedlichen Festigsskaleneffekte existieren.

Die Auswertung der experimentellen Ergebnisse einer grossen Anzahl von Scherversuchen an Modellfugen hat gezeigt, dass eine lineare Relation zwischen dem Grösstvolumenvergrösserungswinkel und dem Grösstspannungsverhältnis existiert. Es wurde ausserdem festgestellt, dass eine einfache Relation zwischen dem Grösstvolumenvergrösserungswinkel und dem Verhältnis der normalen Spannung zur Zylinderdruckfestigkeit besteht.

Eine einfache Methode, um die Rauheitsprofile für Fugen von verschiedenen Rauhigkeiten statistisch zu analysieren, wurde entwickelt. Man muss die Steigung der Unebenheiten für verschiedene Seitenlängen berechnen. Es wurde festgestellt, dass diese Werte analog sind zu den wechselnden Grösstvolumenvergrösserungswinkeln für verschiedene Normalspannungen.

Die praktische Andwendbarkeit dieser Scheranalogie für Böschungsstabiliteitsprobleme ist zusammengefasst, und ein typisches Beispiel wurde durchgerechnet. Die photogrammetrische Aufzeichnung der Fugenrauheit an den zutagetretenden Gesteinsflächen, und die statistische Analyse der Ergebnisse, lässt die Grösstscherfestigkeit für jeden Bereich der Normalspannung bestimmen.

INTRODUCTION.

It is generally acknowledged that the major difficulty in rock mechanics practice is the reliable measurement of relevant field data. There appears to be an ever-widening gap between the quality of this input data, and the numerical methods of analysis currently available. This paper represents an attempt to narrow this gap in one important field.

In the past, attempts have been made to relate the shear resistance of rock joints to the observed dilatent behaviour of granular materials such as sand. From considerations of statics, Newland and Alley (1) developed an equation of the following type:

$$\tau = \sigma \tan(\phi_b + i)$$

to denote the maximum shear strength of a granular mass. The angle (i) was the average angle of deviation of particle displacements from the direction of the applied shear stress, and (ϕ_b) was the angle of frictional sliding resistance between particles. Rowe, Barden and Lee (2) developed the same relationship for cohesionless sands from energy considerations. For the direct shear test the total applied shear force was divided into three components. These took account of the ex-

ternal work done in dilating against the normal force, and the internal work done in overcoming dilational friction which was differentiated from the "no volume change" frictional component. The sum of these three components produced the above relationship.

Patton(3,4) and Goldstein et al. (5) used the same relationship to represent the shear strength of irregular rock surfaces and broken rock when tested at low normal stresses. At high normal stresses it was anticipated that most of the irregularities would be sheared off. Consequently the Coulomb relation was introduced:

$$\tau = c + \sigma \tan \phi$$

where the constants (c) and (ϕ) denote the Coulomb shear parameters relating to the strength of the unjointed rock material. Thus Patton and Goldstein et al. proposed the familiar bi-linear approximation to the anticipated curved strength envelope.

Patton's work provides a simple experimental basis for the development of more fundamental failure models. He performed a series of laboratory shear tests on idealized rock surfaces using kaolinite-plaster specimens having interlocking teeth. Specimens with teeth inclined at 45°, 35° and 25° (of the same height) produced peak strength envelopes which could be approximated to bilinear relationships. The initial linear portions (representing low normal stress) were inclined at 75°, 66° and 55° respectively. The second linear portions were all inclined at 30°, which was the same as the angle of residual friction (i.e. $\phi = \phi_b$ in this instance). The bilinear transition points varied between the three types of specimen, with the 45° toothed surfaces reaching the transition at lower normal stress than the 35° or 25° models. This was obviously a function of the relative base area of the teeth. It was therefore postulated that for a real joint surface the steepest asperities might be sheared off at quite low normal stresses.

Effective (i) value.

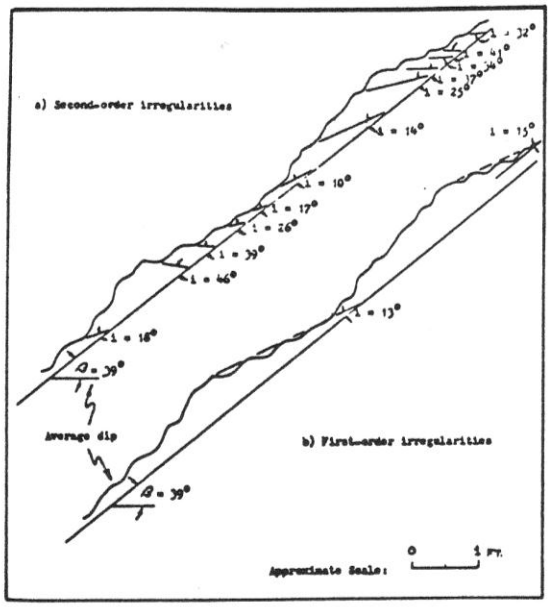

Fig. 1. First and second order irregularities (after Patton (3)).

Erste und zweite Ordnung Unebenheiten (nach Patton (3)).

Irrégularités du premier et second ordre (d'après Patton (3)).

Patton also studied a large number of unstable rock slopes in the Rocky Mountains. Photographic observation and measurement of joint surface profiles, and a related series of residual shear tests on flat, sawn rock specimens led him to the conclusion that first order and second order irregularities of the joint surface had to be differentiated, if realistic strength parameters were to be obtained through back analysis. Figure 1(taken from Patton (3)) demonstrates the significance of the two scales of roughness. In essence his conclusion was that an "effective" (i) value had to be used, rather than the absolute roughness of the small asperities lying on the slopes of the first order irregularities. As far as the author is aware, no method has been suggested for actually recognising the appropriate effective (i) value for a given field problem.

Figure 2 (a) demonstrates the static considerations of sliding up an idealized smooth inclined rock surface which exhibits a basic angle of friction (ϕ_b) the same as the residual angle, and also obtainable from shear tests of flat sand blasted or sawn surfaces of the rock. Equating the resolved components

of H and N for the condition of limiting equilibrium the following familiar relation is obtained:

$$H/N = \tan(\phi_b + i)$$

This is obtained more directly as follows. Sliding is just initiated when the resultant force is inclined at an angle ϕ_b from the normal to the inclined surface. Therefore the tangent of the "total friction angle" is equal to the ratio of H and N.

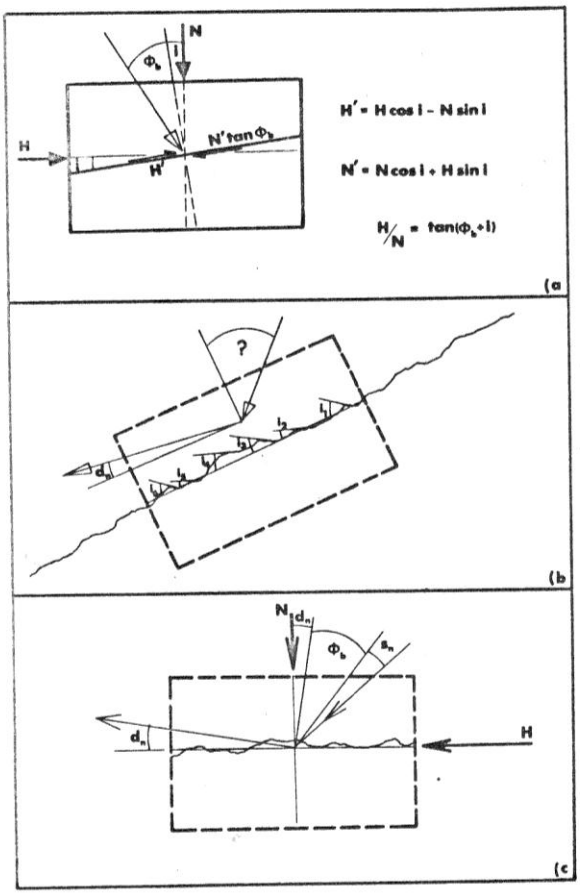

Fig. 2. Three diagrams of joint shear behaviour.

Drei Diagramme über Fugenscherverhalten.

Trois graphiques représentant le comportement au cisaillement.

Peak dilation angle.

The real situation of shearing or sliding along a rough joint is illustrated in diagram (b) of Figure 2. A multitude of (i) values contribute to the peak shear strength, and the effective (i) value will be dependent on the normal stress acting across the joint. It is suggested that at the instant of failure (peak shear strength) the rock mass lying above the joint will move at an angle (d_n) inclined to the mean plane. This is the effective (i) value, but it will now be termed the "peak-dilation angle". It is a very powerful phenomenological parameter of shear strength, since for a given normal stress it represents the minimum energy path between a "sliding up" and a "shearing through" mode of failure.

$$d_n = \text{maximum incremental } \frac{d_v}{d_h}$$

where d_v and d_h are the increments of perpendicular and tangential displacement respectively.

All the two hundred shear tests performed on rough model tension fractures (Barton (6)) demonstrated peak dilation angles corresponding to the shear displacement at which peak strength was mobilized.

Previous measurements of joint dilation.

Ripley and Lee (7) reported an interesting series of direct shear tests on natural discontinuities in sandstone, siltstone and mudstone obtained from 6 inch diameter drill core. Dilation measurements were taken during each test. When expressed in terms of an apparent friction angle, the increase in sliding resistance due to "riding up" on the rough joint projections was found to be from 10° to 18° for the peak values at low strain, and from 2° to 13° for higher strains. It is significant that their total angles of friction at higher strains "corrected" to approximately the residual angle of friction, while the peak values when corrected were somewhat higher than this. For instance for the sandstone specimens:

MEASURED		CORRECTED	
peak	ultimate	peak	ultimate
54°	40°	36°	27°

It was therefore apparent that the dilation "correction" proposed by Skempton and Bishop (8) for direct shear tests on (cohesionless) sands could not be applied to the peak strength state of rock joints. Even at low normal stresses some failure of intact material was occurring at the tips of asperities in contact.

Two further references should be cited from the small amount of rock mechanics literature reporting dilation measurements: Ruiz, Camargo, Midea and Nieble (9) and Tsytovich, Ukhov and Burlakov (10). Both papers refer to in situ tests of concrete-rock interfaces. However, Ruiz et al. also report dilation measurements from a large (375 ft^2 area) in situ shear test of a basalt-breccia contact at a normal stress of only 24 lbf/in^2. Peak dilation angles as high as 39° and 32° were obtained for the undisturbed and first sliding tests.

Component of asperity strength.

The theoretical maximum inclination of a smooth faced asperity which is to remain unsheared when tested at zero normal stress is as follows:

$$(i)_{max} = 90 - \phi_b$$

This is apparent from inspection of the function tan ($\phi_b + i$), and was referred to by Ripley and Lee (7), Withers (11) and Patton (3).

The large amount of experimental data reported in the literature suggests that more or less all rocks have basic angles of sliding friction (ϕ_b) the same as the residual angle, and lying between approximately 25° and 35° (see for instance Ripley and Lee (7), Patton (3), Rosengren (12), Ross Brown and Barton (13)). For this reason smooth asperities inclined at between 55° and 65° to the mean plane may be sheared through even when the test is conducted at a theoretical zero normal stress. Real, rough faced asperities might therefore limit the maximum possible dilation angle to 30° or 40° for this theoretical zero normal stress.

Ladanyi and Archambault (14) proposed a failure model in which the small area of sheared asperity was given a strength component corresponding to the Coulomb relation for shear through unjointed rock. They suggested that over the remaining area of the joint surface, only the frictional and dilational components were acting. This concept is no doubt a valid one, but unfortunately the number of unknown parameters in their relationship was impractically large.

Diagram (c) of Figure 2 illustrates the problem posed by this shear component. Peak strength is reached when the ratio of the shear and normal forces is equal to the tangent of the sum of ϕ_b, d_n and s. The shear component (s) appears to be stress dependent, just as the peak dilation angle (d_n) is inversely.

It will be apparent from this review of joint shear failure concepts that no practical method existed for predicting the peak shear strength envelopes of rock joints. The problem is complicated by an additional unknown; the question of possible scale effects.

Deere, Hendron, Patton and Cording (15) suggested that the strength of laboratory (6 inch), in situ (3 feet) and failure surface (10 to 100's of feet) "specimens" would be mutually different for a wide range of surface profiles. It was thought that because the small specimens could only sample the second and third order scales of roughness, they could not be representative samples of the total failure surface problem. This scale effect was thought to be particularly true of rough undulating tension joint surfaces, and to a lesser degree of smoother surfaced undulating joints or bedding planes. By implication smooth, planar joint surfaces were not expected to exhibit any strength-scale effect.

In direct contrast to these hypoteses should be mentioned the review of in situ shear test experiences by Seraphim and Guerreiro (16). Test areas ranging from 10 ft^2 to 375 ft^2 were considered not to have confirmed any strength-scale effect.

SCALE EFFECTS OF MODEL TENSION JOINTS.

The very weak, brittle model material (Barton (17)) developed during reduced scale (1:500) model studies of the behaviour of excavated rock slopes (Barton (6)) presented an ideal opportunity for studying possible scale effects. This problem had to be assessed before any general strength criterion for rock joints could be formulated.

1. Strength-scale effect.

Four model materials having widely different compressive strengths were used in the investigation. These materials; C2, C4, C9 and C25 were obtained from cured combinations of red lead-sand/ballotini-plaster-water. Different quantities of the cementing component were used to obtain the different strengths.

It was intended to perform all direct shear tests on the same dimension of model tension joint, namely 2.3 inches by 1.0 inch. These were developed by tensile splitting on a specially developed guillotine. If all four model materials were taken to represent the same strength of prototype rock, then by a simple dimensionless relationship, the four model joint types would be simulating four different dimensions of prototype joint surface. The table below summarizes the model-prototype scaling of the four model materials.

Table 1. Model-prototype scaling of four materials.

Model material	σ_c (lbf/in^2)	ρ (lbf/ft3)	λ	ψ	Prototype (feet)	Prototype σ_c
C2	10.2	120.7	500	666	96.0x42.0	6,800 (lbf/in^2) (ALL)
C4	56.2	120.8	91	121	17.5x7.5	
C9	88.8	117.4	56	77	10.7x4.7	
C25	119.0	108.7	38.6	57	7.4x3.2	

where: σ_c is the unconfined compressive strength
ρ is the density
λ is the geometric scale
ψ is the stress scale

A full discussion of model similtude is given by Barton (6).

Each of the four model types was tested at a different range of normal stress (σ_n) such that, when these were converted to prototype stresses, the range for all four was the same and approximately 0 to 1600 lbf/in^2. Figure 3 shows the surfaces of the specimens after shearing. Quite large amounts of damage were noticed on those surfaces which were tested at the highest normal stresses.

The model shear strength envelopes displayed widely different strengths, as would be anticipated from the range of unconfined compression strengths. However, the prototype envelopes shown in Figure 4, show a remarkably small scatter in overall results. (Each plotted point is the mean of two shear tests at the same normal stress). Note in particular the absence of a true "cohesion intercept", even for joints as rough as those tested. The curved shape of the peak envelopes is typical of results of direct shear tests on joints in rock, see for instance Krsmanovic, Tufo and Langof (18).

The closeness of the peak strength results leads one to the conclusion that there may not be a significant strength-size effect for rough tension joints of this type. The apparently more planar profiles of the 7.4 and 10.7 feet simulated joints belie the fact that for many different joint dimensions there is probably a roughness "world within a world". As will be seen later the small steep asperities seem to control the peak strength to a greater degree than the larger amplitude low inclination first order asperities. These only become dominant at normal stress levels considerably higher than encountered in near-surface excavations, or for shear displacements larger than those required to develop peak strength. However, these comments are not

SCALE EFFECTS OF MODEL TENSION JOINTS.

The very weak, brittle model material (Barton (17)) developed during reduced scale (1:500) model studies of the behaviour of excavated rock slopes (Barton (6)) presented an ideal opportunity for studying possible scale effects. This problem had to be assessed before any general strength criterion for rock joints could be formulated.

1. Strength-scale effect.

Four model materials having widely different compressive strengths were used in the investigation. These materials; C2, C4, C9 and C25 were obtained from cured combinations of red lead-sand/ballotini-plaster-water. Different quantities of the cementing component were used to obtain the different strengths.

It was intended to perform all direct shear tests on the same dimension of model tension joint, namely 2.3 inches by 1.0 inch. These were developed by tensile splitting on a specially developed guillotine. If all four model materials were taken to represent the same strength of prototype rock, then by a simple dimensionless relationship, the four model joint types would be simulating four different dimensions of prototype joint surface. The table below summarizes the model-prototype scaling of the four model materials.

Table 1. Model-prototype scaling of four materials.

Model material	σ_c (lbf/in^2)	ρ (lbf/ft3)	λ	ψ	Prototype (feet)	Prototype σ_c
C2	10.2	120.7	500	666	96.0x42.0	6,800 (lbf/in^2) (ALL)
C4	56.2	120.8	91	121	17.5x7.5	
C9	88.8	117.4	56	77	10.7x4.7	
C25	119.0	108.7	38.6	57	7.4x3.2	

where: σ_c is the unconfined compressive strength
ρ is the density
λ is the geometric scale
ψ is the stress scale

A full discussion of model similtude is given by Barton (6).

Each of the four model types was tested at a different range of normal stress (σ_n) such that, when these were converted to prototype stresses, the range for all four was the same and approximately 0 to 1600 lbf/in^2. Figure 3 shows the surfaces of the specimens after shearing. Quite large amounts of damage were noticed on those surfaces which were tested at the highest normal stresses.

The model shear strength envelopes displayed widely different strengths, as would be anticipated from the range of unconfined compression strengths. However, the prototype envelopes shown in Figure 4, show a remarkably small scatter in overall results. (Each plotted point is the mean of two shear tests at the same normal stress). Note in particular the absence of a true "cohesion intercept", even for joints as rough as those tested. The curved shape of the peak envelopes is typical of results of direct shear tests on joints in rock, see for instance Krsmanovic, Tufo and Langof (18).

The closeness of the peak strength results leads one to the conclusion that there may not be a significant strength-size effect for rough tension joints of this type. The apparently more planar profiles of the 7.4 and 10.7 feet simulated joints belie the fact that for many different joint dimensions there is probably a roughness "world within a world". As will be seen later the small steep asperities seem to control the peak strength to a greater degree than the larger amplitude low inclination first order asperities. These only become dominant at normal stress levels considerably higher than encountered in near-surface excavations, or for shear displacements larger than those required to develop peak strength. However, these comments are not

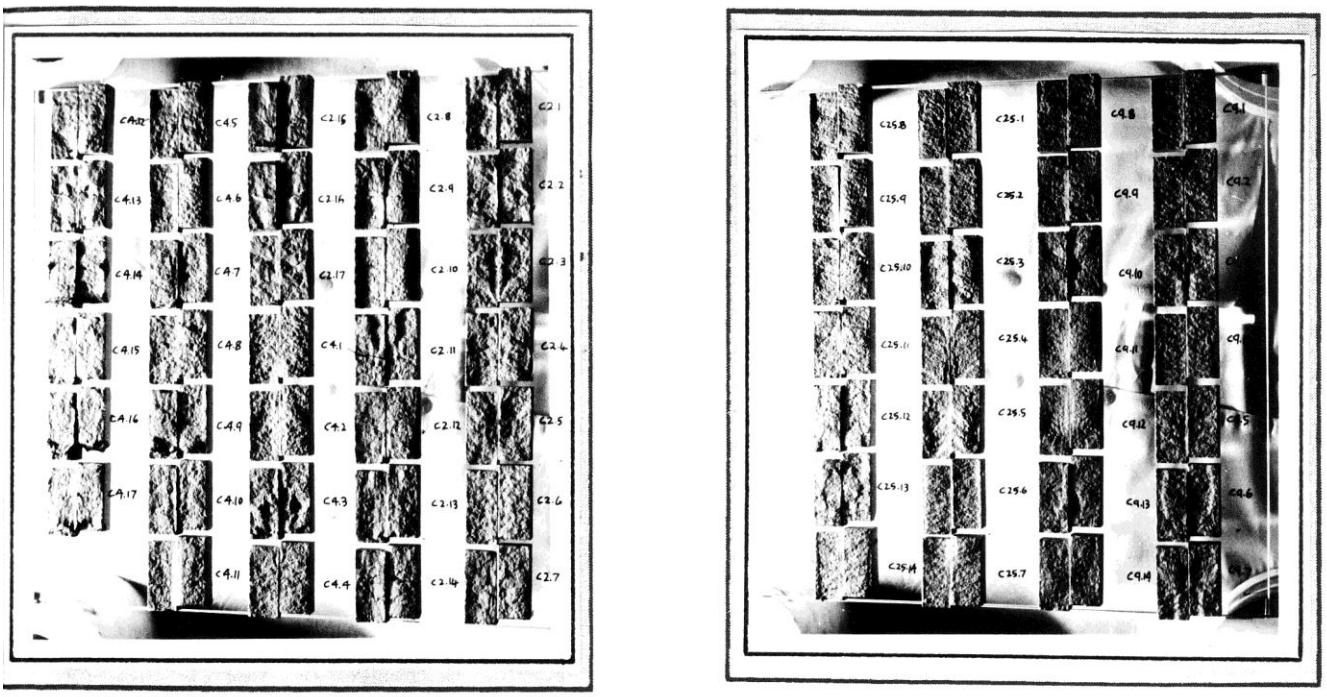

Fig. 3. Examples of model tension joints.

Beispiele von Modellzugfugen.

Exemples de fissures de traction sur modeles.

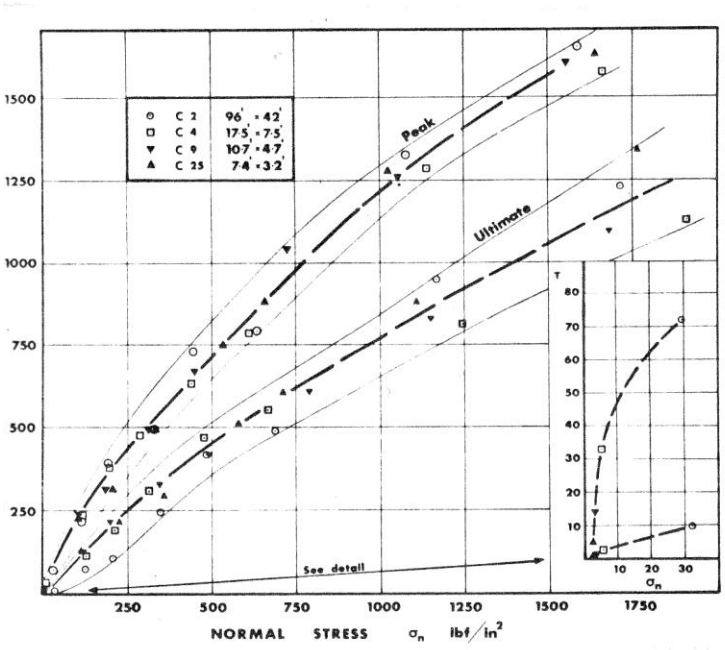

ig. 4. Shear strength at prototype scale.

cherfestigkeit im Prototyp Masstab.

ésistance au cisaillement à l'échelle de rototype.

applicable to severely weathered joints due to the reduced strength of the joint walls, and the resultant damage to larger scale joint features.

2. Displacement-scale effect.

Laboratory size joint specimens (6 to 12 inches long) generally reach peak strength after tangential displacements of small fractions of an inch (Goodman (19)). The largest in-situ tests performed likewise reach peak strength after only ½ to 1½ inches displacement at the very most. The four types of model joints, representing prototype dimensions from approximately 7 to 96 feet in length, provided an opportunity for a comparative study of displacement-scale effects. Table 2 summarizes the prototype values predicted from each scale of model shear test. Each displacement is the mean value of two tests at the same normal stress.

Table 2. Prototype displacements extrapolated from four model materials.

NORMAL STRESS				DISPLACEMENT							
σ_n (lbf/in^2)				d_h peak (ins)				d_v peak (ins)			
C2	C4	C9	C25	C2	C4	C9	C25	C2	C4	C9	C25
29	5.3	3.4	2.5	3.35	0.54	0.35	0.34	-	-	-	-
112	115	110	109	5.12	1.40	0.71	0.55	2.30	0.15	0.11	0.06
190	196	184	207	5.32	1.04	0.66	0.70	1.65	0.13	0.06	0.06
318	288	316	327	8.46	1.40	0.71	0.46	0.75	0.09	0.06	0.03
445	439	449	535	9.45	1.36	0.71	0.93	0.25	0.17	0.04	0.07
635	611	726	658	11.61	1.36	0.75	1.05	0.45	0.13	0.09	0.08
1079	1140	1058	1026	9.65	2.37	0.91	0.79	-0.05	0.25	0.15	0.17
1588	1661	1551	1640	8.85	1.40	0.64	1.03	-0.10	0.16	0.07	0.05

The symbols used in the tabulation represent the following:

d_h peak: is the tangential displacement at peak shear strength

d_v peak: is the perpendicular displacement at peak shear strength.

It would appear from the results that there may be a marked displacement-scale effect for rough tension joints of this type. The peak strengths were reached after tangential displacements approximately 1% of the lengths of the joints tested, whether these simulated 96 feet or only 7.4 feet at full scale.

The ultimate tangential displacements were the same for each model and represented 7.7% of the length of each simulated test dimension. From an examination of the drop from peak strength towards residual strength, it would appear that a displacement of approximately 10% would reduce the shear strength of similar rough joints to close to the residual strength.

OBSERVATIONS OF ASPERITY FAILURE DURING SHEAR.

Figure 5 is a photograph of twenty model joint surfaces representing seven types of joint. Each specimen is one of a mating pair photographed before shear testing and later aligned in the shearbox in a known direction. The roughness profiles (elevations) superimposed on these photographs were obtained from a photogrammetric analysis of the surfaces (see Wickens and Barton (20)). Approximately 70 spot height coordinates were computer-plotted for each of the two profiles per surface. These were taken longitudinally along the two third points of the 2.3 inches by 1.0 inch model joints.

As a preliminary to detailed analysis of the roughness profiles, some of the shear tests performed on the joints shown in Figure 5 were "reconstructed", so that the effect of normal stress on asperity failure could be assessed. Figures 6 and 7 show the experimental shearing paths measured during the relevant tests, superimposed on the related pairs of roughness profiles for the two joints concerned. Both the joints chosen for this example were in model material C2(P), representing a prototype unconfined compression strength of 6,800 lbf/in^2 and a joint length of 96 feet.

Detailed observations of these sequences were given by Barton (6). For the present the following conclusions can be drawn. (Note that sequence No. 2 represents peak strength in each case).

1. The test representing a low normal stress (112 lbf/in^2, Figure 6) showed face to face joint contact at only the steepest points of the asperity tips, with very little asperity shear (black overlapped zones).

2. The test representing a high normal stress (635 lbf/in^2, Figure 7) showed appreciable areas of contact due to the lower inclination of asperity that was being sheared through at the higher stress.

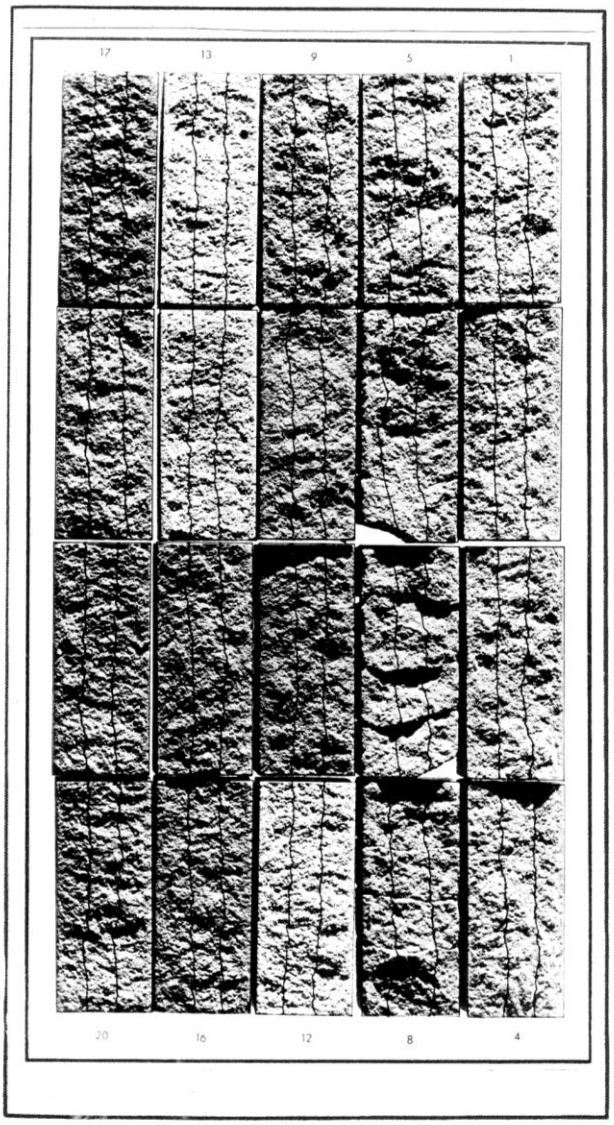

Fig. 5. Photogrammetric roughness profiles.

Photogrammetrische Rauheitsprofile.

Représentation photogrammétrique de profils de rugosité.

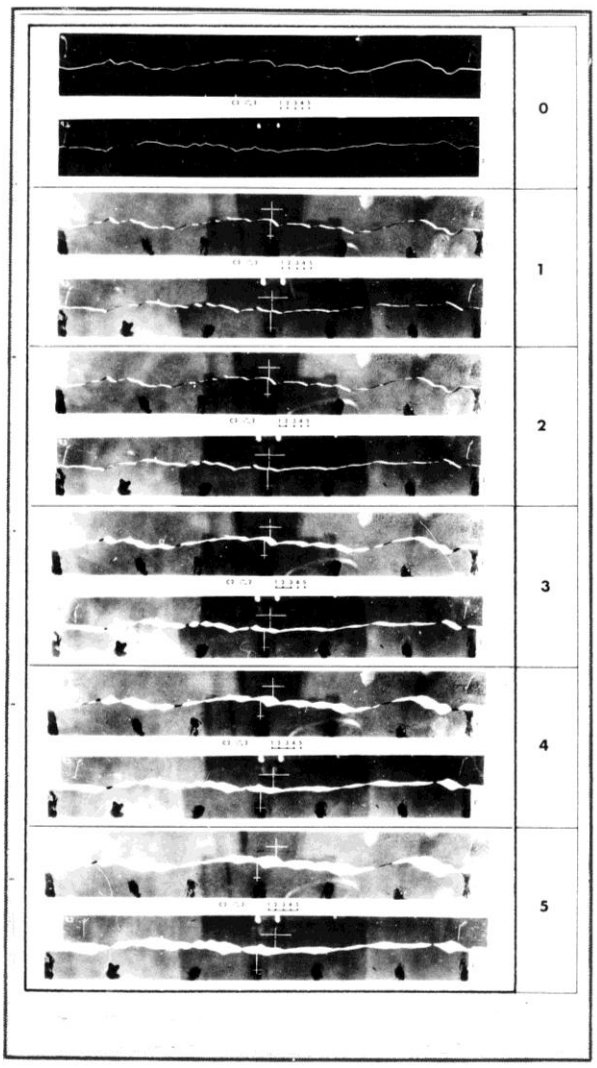

Fig. 6. Reconstructed shear test: low normal stress.

Rekonstruierter Scherversuch: niedrige Normalspannung.

Essai de cisaillement reconstruit: faible tension normale.

TWO EXPERIMENTAL RESULTS FOR MODEL TENSION JOINTS.

1. Relationship between peak stress ratio and peak dilation angle.

Peak dilation angles and corresponding ratios of (τ/σ_n) at peak strength were calculated for eight different types of model joint. These ranged from the rough interlocking "secondary" joints C3(S) (specimens 6, 7 and 8 of Figure 5), down to the more regular "primary" joints of C25(P). (C25. 1 to 14 of Figure 3, specimens 12, 13 and 14 of Figure 5). In addition, some experimental data for tension fractures in Blackstone granite were kindly supplied by De Freitas (21).

The distribution of data for arctan $(\tau/\sigma_n)^\circ$ versus $(d_n)^\circ$ is shown in Figure 8. Each model result is the mean of two tests at the same normal stress. A least squares analysis was carried out, and gradients and intercepts calculated for the best fit straight lines to each of the eight model joint types, and also to the total

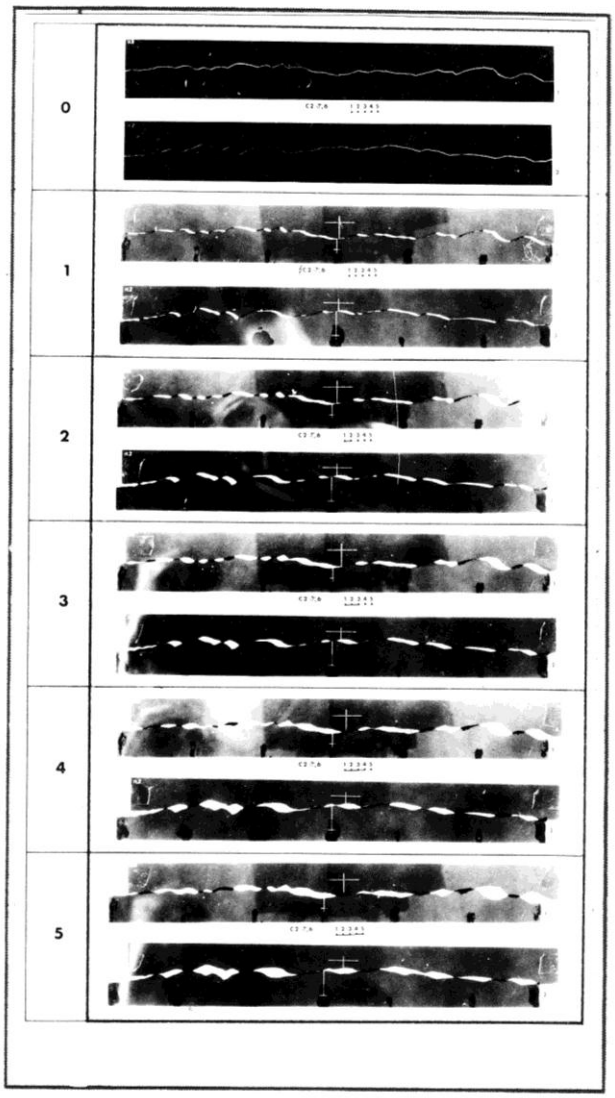

Fig. 7. Reconstructed shear test: high normal stress.

Rekonstruierter Scherversuch: hohe Normalspannung.

Essai de cisaillement reconstruit: tension normale élevée.

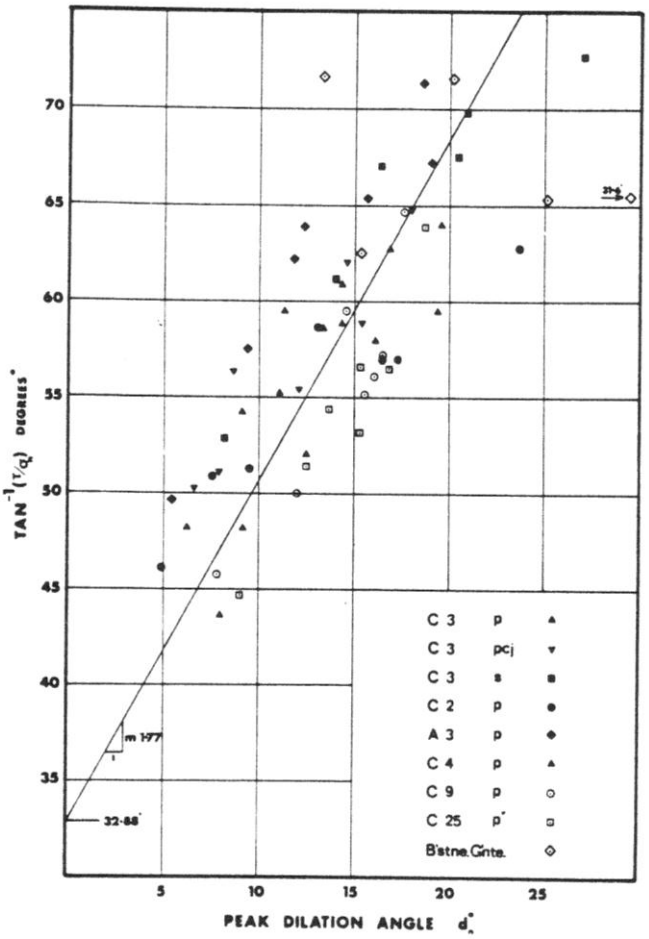

Fig. 8. Linear variation of peak delation angle with peak stress ratio.

Lineares Verhältnis des Grösstvolumenvergrösserungswinkels mit dem Grösstspannungsverhältnis.

Variation de l'angle maximum de dilatation en fonction du rapport de contraintes maximum.

sample. The model results were doubly weighted compared to the single tests on granite, and the peak dilation angle (d_n) was taken as the dependent variable. The following table gives the result of this analysis:

Joint type	Gradient (M)	Intercept (C)
C3(S)	1.16	44.4°
A3(P)	1.50	42.7°
C2(P)	0.92	42.6°
C3(P)	1.28	40.6°
C3(PCJ)	1.34	41.0°
C4(P)	1.91	30.0°
C9(P)	2.04	26.2°
C25(P)	1.94	26.2°

The following result was obtained for the total weighted sample:

$$\tau/\sigma_n = \tan\,(1.78\ d_n + 32.88^\circ)$$

Three important observations should be noted:

1. The tabulation is arranged in decending order of joint roughness, as far as this is possible from a visual examination of the surfaces.

2. If (d_n) is put equal to the intercept (C) in the above equation the function (MC+C) is equal to 89.6°.
3. If this is done for all the model joint types presented in the table, a mean value of (MC+C) equal to 91.3° is obtained.

Bearing in mind the variety of joint surfaces, and the experimental scatter of results, it was felt that the least squares fit to the whole test sample represented the most reliable basis for any general strength criterion. The intercept of 32.88° was fortuitously close to the basic angle of friction of the model materials (range 28½° to 32°), and this suggested the following peak strength criterion:

$$\tau/\sigma_n = \tan\left[\left(\frac{90-\phi_b}{\phi_b}\right)d_n + \phi_b\right] \qquad (1)$$

when ϕ_b is 30° this reduces to the simple form:

$$\tau/\sigma_n = \tan\left[2d_n + 30^\circ\right] \qquad (2)$$

2. The relationship between normal stress and peak dilation angle.

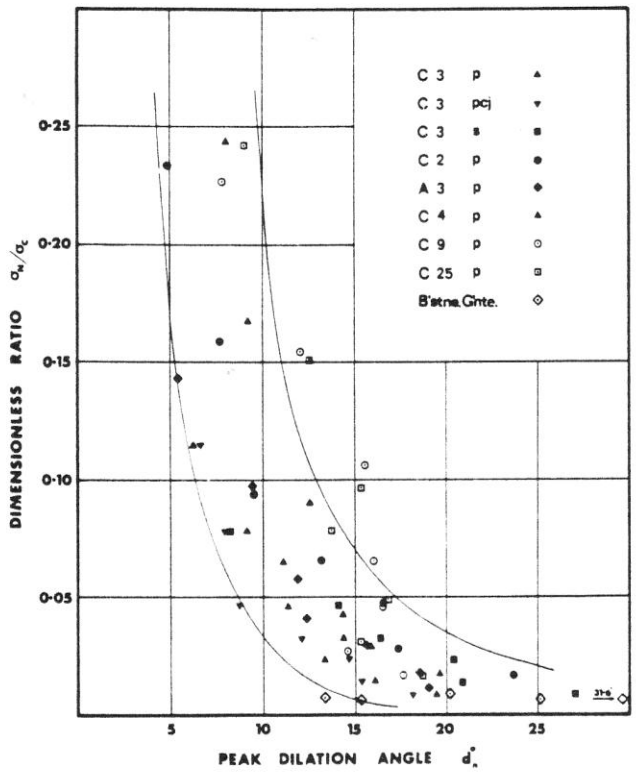

Fig. 9. Variation of peak dilation angle with ratio of normal stress to compressive strength.

Änderung des Grösstvolumenvergrösserungswinkels mit dem Verhältnis der Normalspannung zur Zylinderdruckfestigkeit.

Variation de l'angle maximum de dilatation en fonction du rapport contrainte normale / force de compression.

The model joints were tested at a variety of normal stress levels, depending upon the relative compressive strengths of the materials concerned. Mutual comparison was therefore only possible when the normal stresses were normalized (see for instance Hoek (22)) by dividing by the appropriate unconfined compression strengths. The dimensionless plot of (σ_n/σ_c) versus peak dilation angle (d_n) could then be compared with data for rock. (None appears to have been reported to date).

Figure 9 shows the curved trend of this experimental data. A linear relationship was obtained when the data was replotted with the dimensionless ratio (σ_n/σ_c) on a logarithmic scale Figure 10). A least squares fit to the total weighted sample gave the following equation:

$$\log_{10}(\sigma_n/\sigma_c) = -0.1056\, d_n + 0.1184$$

It was noticed that only a very small rotation was required to produce the simple form:

$$\log_{10}(\sigma_n/\sigma_c) = -0.100 d_n$$

or

$$d_n = 10 \log_{10}(\sigma_c/\sigma_n) \qquad (3)$$

σ_c/σ_n	d_n
1.0	0°
10	10°
100	20°
1000	30°

The simplicity of this relationship suggests that the result may be most significant to an understanding of tension joint behaviour:

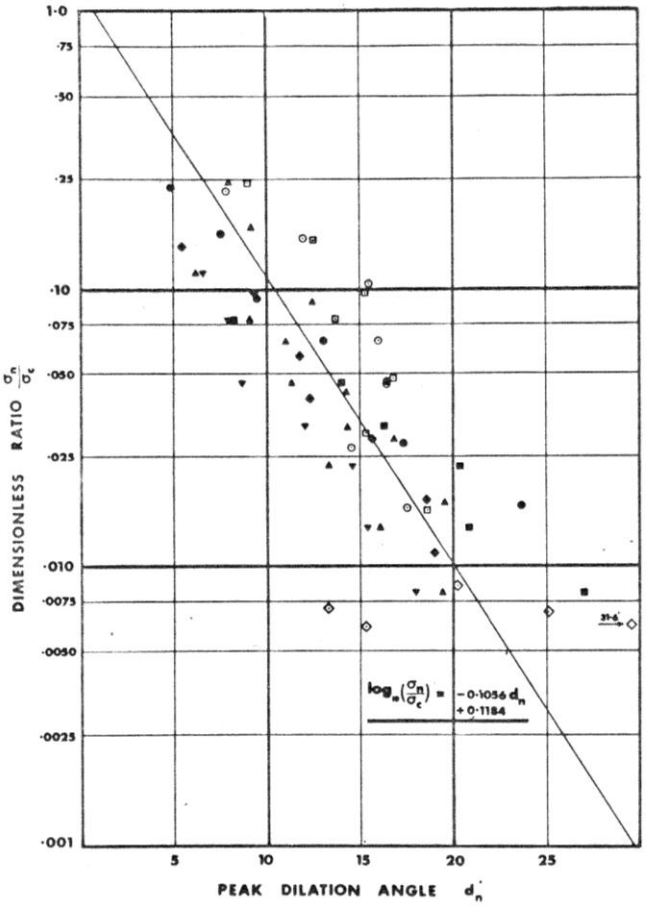

Fig. 10. Linear variation of peak dilation angle with logarithmic ratio of normal stress to compressive strength.

Lineare Änderung des Grösstvolumenvergrösserungswinkels mit dem logarithmischem Verhältnis von Normalspannung zur Zylinderdruckfestigkeit.

Variation linéaire de l'angle maximum de dilatation en fonction du rapport logarithmique contrainte normale / force de compression.

GENERAL CRITERION OF PEAK STRENGTH FOR ROUGH JOINTS.

When equation 3 is combined with equation 2 to eliminate (d_n), a very useful general criterion of peak strength is obtained:

$$\tau/\sigma_n = \tan\left[20\log_{10}\left(\frac{\sigma_c}{\sigma_n}\right) + 30^\circ\right] \quad —(4)$$

This would seem to have application in situations where the joint surface was statistically unknown, but sufficiently rough to bear comparison with the model tension joints. It can be applied to practical situations in two ways:

1. Unweathered tension joints.
The peak shear strength (τ) for unweathered tension joints in rock can be estimated from a knowledge of the unconfined compression strength of the rock concerned.

For example: the design chart shown in Figure 11 indicates that a rock of 10,000 lbf/in^2 in unconfined compression, when shear tested at a normal stress of 200 lbf/in^2 (σ_c/σ_n = 50) would give a ratio of peak (τ/σ_n) of approximately 2.06. Thus for a range of normal stresses the desired peak strength envelope could be estimated.

2. Weathered tension joints.
Weathered tension joints in rock present a more difficult problem since the unconfined compression strength of the sound rock cannot be easily related to the "effective joint wall compressive strength" (JCS) of the weathered material. Consequently the best approach here would be to perform a limited series of shear tests (in situ if possible) all at the same normal stress. The mean value of peak (τ/σ_n) obtained from these tests could then be used in the design chart.

For example: suppose the mean value of peak (τ/σ_n) was 1.27 for a mean normal stress of 200 lbf/in^2. Figure 11 indicates that the ratio of (σ_c/σ_n) would be approximately 12. This implies a JCS value of 2500 lbf/in^2; a quarter of the previous value. This value could then be used to estimate the peak strength envelope for the normal stress range required.

The shape of the dimensionless relationship between (τ/σ_c) and (σ_n/σ_c) is shown in Figure 12. Practical application of the above methods to slope stability problems is reported under Theme 2 of this symposium. (Barton (23)).

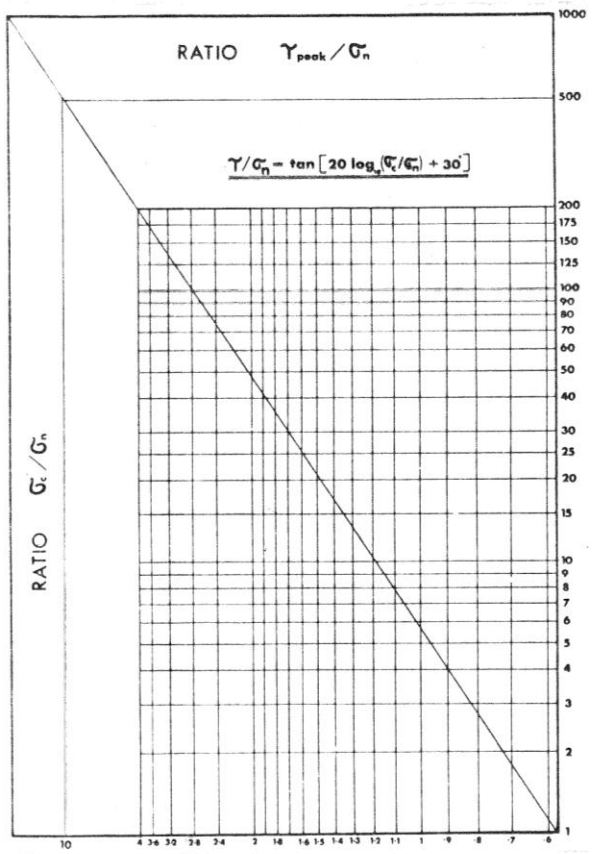

Fig. 11. Design chart for general criterion of peak shear strength.

Entwurfstafel fürallgemeine Kriteria der Grösstscherfestigkeit.

Tableau du critère général de la résistance maximum au cisaillement.

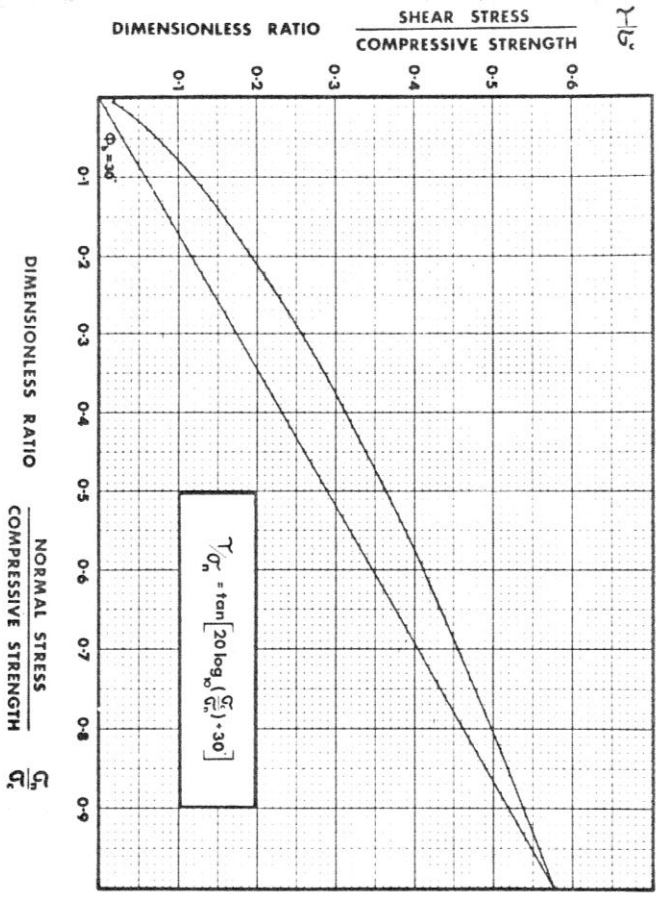

Fig. 12. The shape of the general criterion in dimensionless form.

Die Form des allgemeinen Kriterions in dimensionsloser Anordnung.

La forme du critère général en disposition non dimensionnelle.

MODIFIED PEAK STRENGTH CRITERION FOR JOINTS OF KNOWN ROUGHNESS.

Equation 4 has been briefly demonstrated as a general criterion for peak strength of rough tension joints. However, it is inflexible in that no account can be taken of joints of different degrees of roughness, should these be known.

The gradients and intercepts of the function:

$$\arctan(\tau/\sigma_n) = Md_n + C$$

were presented earlier for all eight different model joints. These values were obtained from least squares analyses, and were tabulated as far as possible in decending order of joint roughness. It will be recalled that the mean value of the relation (MC+C) for individual model joints was 91.3°, and for the whole weighted sample; 89.6°. This implies that the gradient M has the value given in Figure 13. Thus:

$$MC+C = \frac{(90-C)}{C} C + C = 90^\circ$$

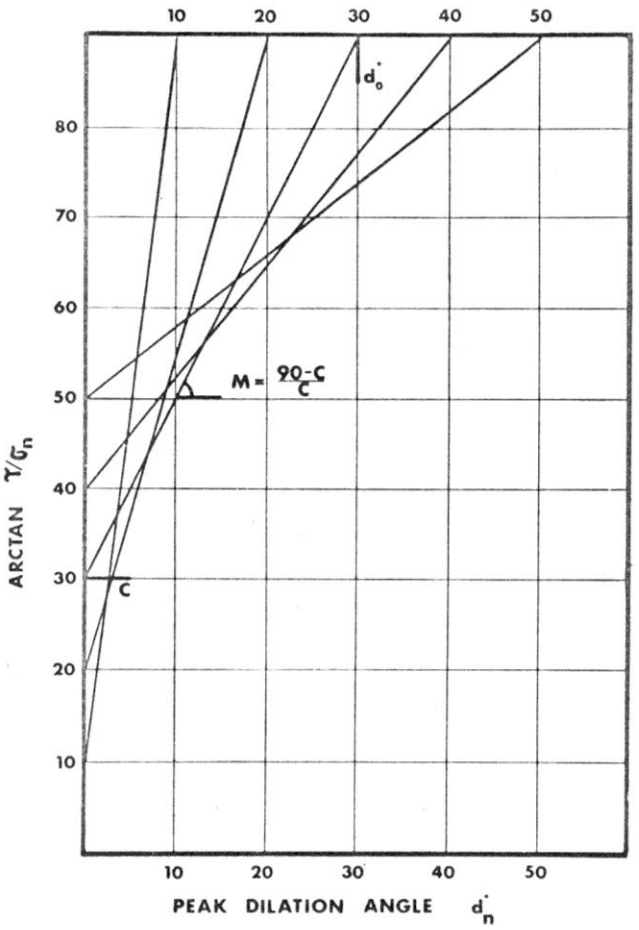

Fig. 13. The relationship of gradients and intercepts.

Die Relation der Gradienten und Abschnitte.

Relation entre gradients et sections.

By implication, the maximum possible dilation angle occurs when arctan (τ/σ_n) is equal to 90°, and its value is equal to the intercept C. Figure 10 shows that the "maximum" dilation angle (29.6^o) occurs when the normal stress is extremely low ($\sigma_n/\sigma_c = 0.001$), and that the intercept C represents the value of arctan (τ/σ_n) when the normal stress is extremely high ($\sigma_n/\sigma_c = 1.0$, $d_n = 0^o$).

Least squares analyses were performed on the logarithmic-linear data of Figure 10 for the eight individual model joint types. The intercepts of "maximum" dilation angle ($d_o{}^o$) for extremely low normal stress ($\sigma_n/\sigma_c = 0.001$) showed a remarkable similarity to the C intercept values obtained previously. The best five pairs of results are given below, once again in decending order of roughness:

Joint	C^o	$d_o{}^o$
C3 (S)	44.4	43.1
C2 (P)	42.6	41.5
C4 (P)	30.0	30.9
C9 (P)	26.2	26.3
C25(P)	26.2	27.3

Thus for the range of normal stress:

$$\sigma_c > \sigma_n > \sigma_c/1000$$

and assuming the intercept (C^o) is very nearly identical to ($d_o{}^o$) for a given surface, the following modified criterion of peak shear strength is indicated:

$$\tau/\sigma_n = \tan\left[\frac{(90-d_o)}{d_o}d_n + d_o\right] \qquad (5)$$

It now remains to statistically analyse the roughness profiles of the model joints, and attempt to find a method for estimating the "maximum" dilation angle ($d_o{}^o$) of a joint surface, and the stress dependent peak dilation angle ($d_n{}^o$).

A STATISTICAL ANALOGY FOR SHEAR BEHAVIOUR OF JOINTS.

The reconstructed shear tests illustrated in Figures 6 and 7 indicated the following:

1. At low normal stress only the steep tips of asperities were sheared through. Thus only a small asperity base length (area) was involved.
2. At higher normal stress less steep asperities with longer base lengths were sheared through.
3. The higher the normal stress the smaller the angle of peak dilation.

The forty roughness profiles illustrated in Figure 5 were available in the form of large scale computer plots (four are shown in Figure 14) and also as spot height coordinates recorded on punch tape. It was appreciated that the positive (and negative) angles between consecutive coordinates represented extremely steep effective (i) values. However, the positive (or negative) angles between every second or third

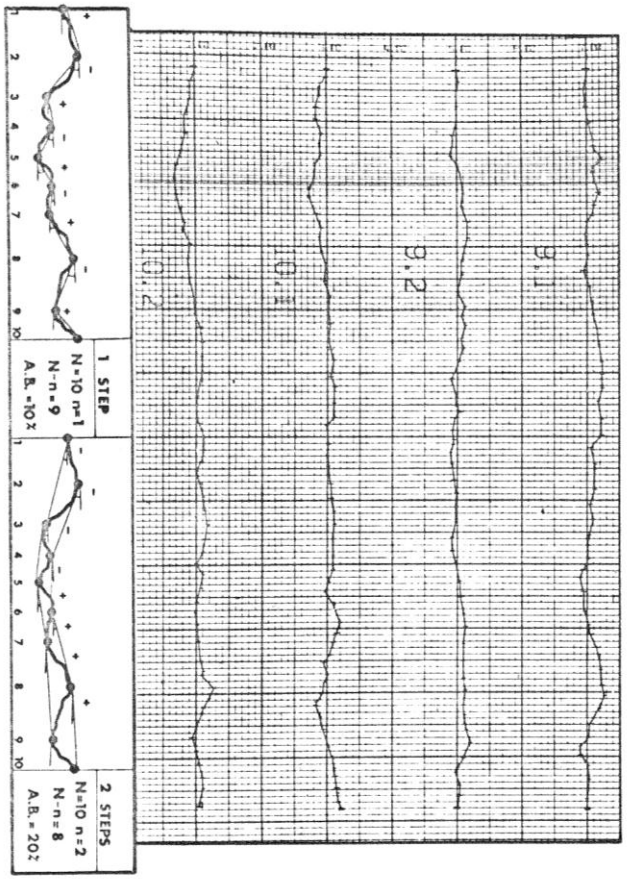

Fig. 14. The analysis of computer drawn roughness profiles.

Die Auswertung der komputergezeichneten Rauheitsprofile.

Analyse de profils de rugosité établis par ordinateur.

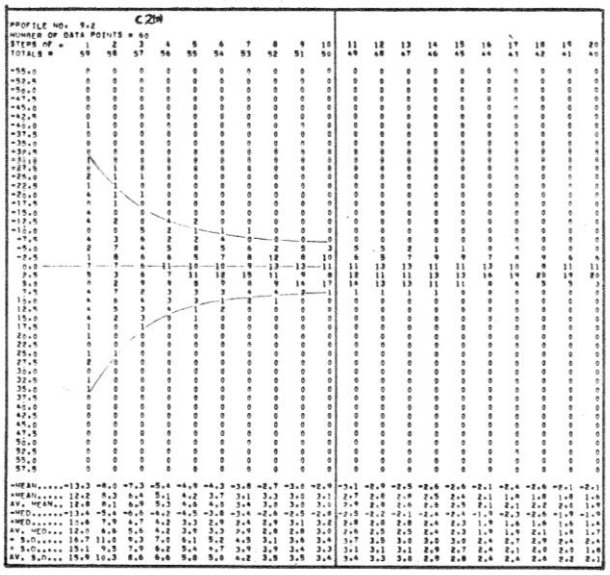

Fig. 15. Typical computer output from statistical analysis.

Typischer Computer Output der statistischen Auswertung.

Résultat typique d'une analyse statistique par ordinateur.

coordinate represented appreciably smaller values. Thus in a crude way the shearing path of joints was simulated by (i) values of different base lengths. The longer the base length the lower the effective (i) value, corresponding to shear through larger asperities at higher normal stresses.

A logical relationship was required between the two pairs of parameters:

1. normal stress — dilation angle
2. asperity base length — effective roughness (i) values.

Input data.

The following computations were required (see Figure 14):

(a) inclination between sucessive coordinates shifting one step at a time. N coordinates, N-1 data points.

(b) inclination between every n th. coordinate, shifting one step at a time. N coordinates, N-n data points.

The majority of profiles were composed of approximately 65 coordinates. (N=65). Steps were taken at coordinate intervals from 1 to 10 (n=1 to 10). The ratio n/N was defined as follows:

$$n/N \times 100\% = \text{asperity base } \% \text{ (A.B.\%)}$$

A similar technique was used by Rengers (24). His "stepsize" was equivalent to the above asperity base.

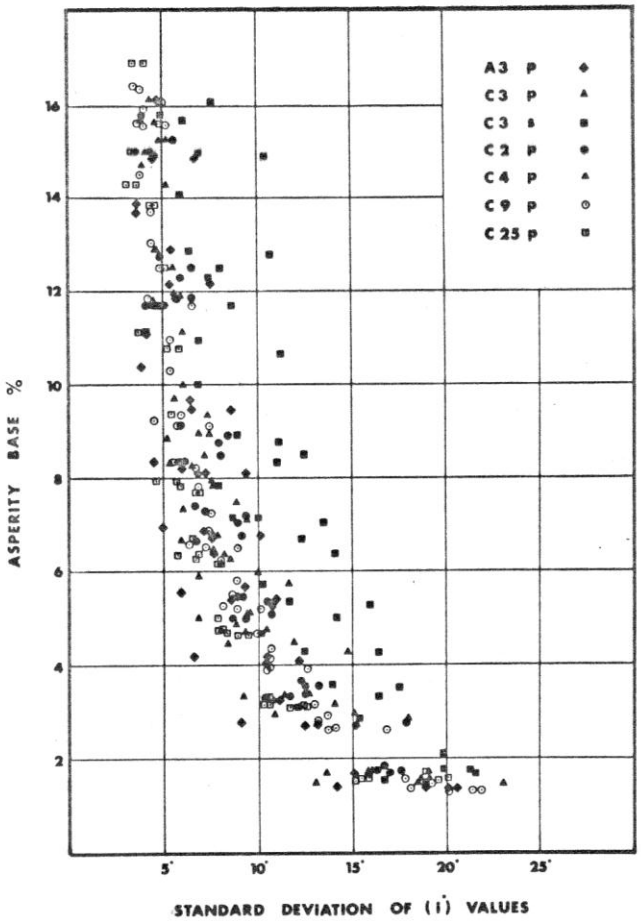

Fig. 16. The results from seven types of model joints.

Die Ergebnisse von sieben Typen von Modellfugen.

Résultats de sept types de modèles de fissures.

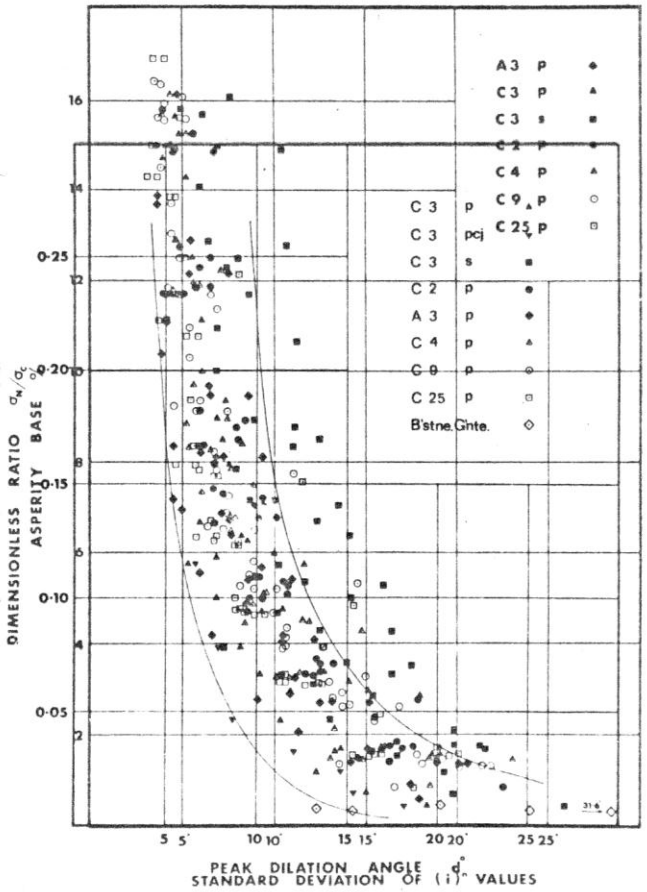

Fig. 17. A statistical shearing analogy.

Ein statistisches Scheranalog.

Une analogie statistique de cisaillement.

Output data.

The forty available profiles with approximately 65 coordinates each, represented a very large number of computations. Consequently a computer programme was developed (Cundall (25)) to produce the following output in the form of histograms:

1. No. of observations for a particular effective (i) value. (Positive and negative angles within the range 0° to 55° for intervals of 2.5^{o}).
2. The same data for different asperity bases. (Steps of 1 to 10).

A typical compound histogram is shown in Figure 15. (It relates to the lower of the pair of profiles shown in Figure 6). For each histogram at each asperity base, the statistical mean, median and standard deviation were computed. This output was divided into positive, negative and average values.

Relationship between asperity base (A.B.%) and standard deviation of (i) values. (S.D.i°).

Figure 16 illustrates the distribution of average S.D.(i)°values for the lower range of asperity bases. The squares representing material C3 (S) were widely separated from the main body of the results because of the offset, stepped nature of secondary joints compared to the continuous primary joints denoted by suffix (P).

Shearing analogy.

The standard deviation of the (i) values is the position on a histogram for a particular asperity base, such that 67% of the observations lie below the S.D.(i) value, and 33% above it. Viewed as a shearing analogy, the 33% of observations of steeper (i) values are "sheared" through, while the 67% of shallower angles remain "unsheared".

The distribution of data shown in Figure 16 was found to be very similar to that of (σ_n/σ_c) versus (d_n) given in Figure 9. Figure 17 shows these two plots overlapped, but slightly offset, for visual comparison. It should be noted that the ordinate A.B.% is exactly half the scale of the ordinate (σ_n/σ_c), when the latter is converted into a percentage. The scales of the two abscissa; peak dilation angle (d_n) and standard deviation of (i) values are identical.

The angle S.D.$(i)^o$ and the base length A.B.% represent only the up-slope of an imaginary controlling "asperity", which just remains unsheared at the normal stress simulated. By doubling this base length the whole controlling "asperity" is simulated. In other words asperity base (A.B.%) is really a misnomer since, as calculated, it is only half a real asperity base. It can be concluded from Figure 17 that the following are useful approximations:

$$1.\quad (\sigma_n/\sigma_c) \times 100\ (\%) = 2 \times \text{A.B.}\ (\%)$$
$$2.\quad d_n = \text{S.D.}\ (i)^o \qquad (6)$$

The statistical data shown in Figure 16 was analysed in the same way as the experimental data given in Figure 10. The logarithmic-linear relationship for A.B. (%) versus S.D.(i) for all seven model joint types gave the following intercepts:

1. A.B.(%) equal to 50% (antilog. 1.7) for S.D.$(i)^o$ equal zero.
2. S.D.$(i)^o$ intercept of 27.3^o for A.B.(%) equal to 0.05% (antilog $\bar{2}.70$).

These should be compared with the experimental intercepts given previously:

1. (σ_n/σ_c) equal to 1.0 (100%) for $(d_n)^o$ equal zero.
2. "Maximum" dilation angle d_o^o equal to 29.6^o for (σ_n/σ_c) equal to 0.001 (0.1%).

The final point to be verified was whether this statistical shearing analogy was sensitive to the different roughnesses of the joint surfaces. Best fit straight lines to the data of individual model joints were studied, and it was found that the intercept values of standard deviation of (i) values for an asperity base of 0.05% compared very favourably with the "maximum" dilation angles for a ratio of normal stress to compressive strength of 0.1%. Once again, as a concession to the inevitable scatter of results only the best five pairs out of seven will be compared:

Joint type	S.D.$(i)^o$ degrees (at A.B.=0.05%)	$d_n^o(=d_o^o)$ degrees (at σ_n/σ_c= 0.1%)
C3(S)	40.8^o	43.1^o
C3(P)	27.6^o	28.8^o
C4(P)	28.7^o	30.9^o
C9(P)	26.0^o	26.2^o
C25(P)	24.4^o	27.3^o

It can be seen that the shearing analogy enables prediction of the "maximum" angle of dilation to be made to within one or two degrees at best. Real situations involving rock joints would obviously produce a wide scatter of results, and the only solution to this would be large numbers of observations of roughness. A statistically viable sample could then be analysed on the basis of probabilities.

PRACTICAL APPLICATION TO SLOPE STABILITY.

Excavation of slopes in a rock-mass which has relatively widely spaced joints, and basically competent rock between the joints, can be expected to induce a translational type of failure if adversely dipping joints are present. The above shearing

analogy can be readily applied to these situations, and the steps involved can be summarized as follows:

1. Estimate the dimensions of the problem of concern (bench stability or complete slope stability), and the consequent range of normal stresses acting across the adversely orientated joints. The normal stress range would usually be calculated from self weight stress assumptions.
2. Estimate the down-dip length of the potential shear surface, which is to be designed against.
3. Estimate the effective joint wall compressive strength (JCS value).

There are two test methods which could be used to obtain this mechanical property:

(a) Point load tests on cylindrical specimens cored through the weathered rock adjacent to the joints. This is a quick and cheap method which can be performed in the field. It appears from a recent study that it may also be a more reliable test method than unconfined compression (see Broch (26), and Franklin, Broch and Walton (27)). The value of (σ_c) can be obtained from the point load strength index by a simple conversion factor, which depends on the diameter of the rock core.

(b) A limited number of direct shear tests on representative joint specimens, loading all at the same normal stress. Application of the design chart (Figure 11) will then give an approximate value of (σ_c) based on the general criterion for rough tension joints (equation 4).

Suppose the following values were obtained for the above estimates:

1. Normal stress range of relevance to the problem 0 to 250 lbf/in^2.
2. Length of potential shear surface: 400 feet.
3. Effective joint wall compressive strength: 5000 lbf/in^2

Therefore (σ_n/σ_c) range = 0 to 5%
and A.B. (%) range = 0 to 2.5% (0 to 10 feet)

(It is of interest that the range 0 to 10 feet required for statistical analysis in this example corresponds to the range of dimensions generally employed in in situ direct shear tests).

The "maximum" dilation angle d_o^o (see equation 5) for a particular joint surface is estimated from the following relationship:

$$d_o^o = S.D.(i) \text{ for A.B.\% of } 0.05\%$$

In the numerical example, 0.05% of 400 feet is 0.2 feet. Therefore it can be seen that statistical analyses of (i) values are required for asperity base steps of:

1. 0 to 10 feet to obtain a range of d_n^o values.
2. 0.2 feet for a specific value of d_o^o.

Evaluation of (τ/σ_n) for a range of normal stresses is achieved by using equation 5 and the two identities given by equations 6.

Field measurement of (i) values.

A stereogrammetric method of (i) value measurement is clearly the simplest and cheapest technique. Wickens and Barton (20) discussed the phototheodolite survey method in some detail, and this will not be described here. It can be seen that stereoscopic pairs of photographs will need to be exposed from two distances from the rock face; firstly to obtain stereoscopic overlap for as many joint exposures larger than 10 feet as possible (coarse survey), and secondly for a fine survey of small scale joint features.

CONCLUSIONS.

1. The results of direct shear tests on model tension joints of different simulated dimensions suggest that there may not be a significant peak-strength scale-effect for tension joints in rock. However, a marked displacement scale-effect is indicated.
2. The general criterion of peak shear strength represents a useful method for estimating the shear strength of a rough joint surface from a knowledge of the effective

joint wall compressive strength. It can also be usefully employed to extrapolate limited shear test data, such as that obtained from the back analysis of rock slope failures (see Barton (23)).

3. A statistical shearing analogy has been discovered; the standard deviation of inclination angles for asperities of different base lengths are analogous quantitites to the experimental values of peak dilation angles for shear tests at different normal stresses.

4. The modified criterion of peak shear strength represents a realistic equation which is sensitive to joints of different degrees of roughness and weathering, dividing rocks of different compressive strengths.

5. The recording and analysis of joint roughness profiles prior to shear testing should ideally become standard procedure, both in the field and in the laboratory (see Rengers (24)). Only then can the potential of the above methods be evaluated, one way or the other.

Acknowledgements.

The author is indebted to Mr. Ernie Wickens and Mr. Don Proctor of the Photogrammetry Department, University College, London, for carrying out all the photogrammetric work reported herein. Sincere thanks are also due Mr. Peter Cundall and Mr. Jim Markland of the Rock Mechanics Department, Imperial College, for their kind advice and computing expertise.

REFERENCES.

1. Newland, P.L. and Allely, B.H. Volume changes in drained triaxial tests on granular materials. Géotechnique. 1957. Vol. 7. No. 1, pp. 17-34.

2. Rowe, P.W., Barden, L. and Lee, I.K. Energy components during the triaxial cell and direct shear tests. Géotechnique. 1964. Vol. 14, No. 3, pp. 247-261.

3. Patton, F.D. Multiple modes of shear failure in rock and related materials. University of Illinois. Ph.D. Thesis. 1966.

4. Patton, F.D. Multiple modes of shear failure in rock. Proc. 1st. Cong. Int. Soc. Rock Mech. Lisbon 1966. Paper 3.47. Vol. 1, pp. 509-513.

5. Goldstein, M., Goosev, B., Pyrogovsky, N., Tulinov, R and Turovskaya, A. Investigation of mechanical properties of cracked rock. Proc. 1st Cong. Int. Soc. Rock Mech. Lisbon 1966. Paper 3.49. Vol. 1, pp. 521-524.

6. Barton, N.R. A model study of the behaviour of steep excavated rock slopes. University of London. Ph.D.Thesis. 1971.

7. Ripley, C.F. and Lee, K.L. Sliding friction tests on sedimentary rock specimens. 7th. Int. Cong. Large Dams. Rome 1961. IV pp. 657-671.

8. Skempton, A.W. and Bishop, A.W. Measurement of shear strength of soils. Discussion by A.W.Bishop. Géotechnique 1950. Vol. 2. No. 2, p.113.

9. Ruiz, M.D., Camargo, F.P., Midea, N.F. and Nieble, C.M. Some considerations regarding the shear strength of rock masses. Int. Symp. Rock Mech. Madrid 1968. II.5, pp. 159-169.

10. Tsytovich, N.A., Ukhov, S.B. and Burlakov, V.N. Failure mechanism of a fissured rock base upon displacement of a loading plate. Proc. 2nd. Cong. Int. Soc. Rock Mech.
Belgrade 1970. Paper 3-13. Vol. 2.

11. Withers, J.H. Sliding resistance along discontinuities in rock masses. University of Illinois. Ph.D.Thesis 1964.

12. Rosengren, K.J. Rock mechanics of the Black Star Open Cut, Mount Isa. Australian National University. Ph.D.Thesis 1968.

13. Ross Brown, D.M. and Barton, N.R. Rock mechanics considerations and the stability of the opencast mines at Rio Tinto, Spain. Imperial College. Rock Mech. Res. Rept. No. D.7 1969, pp. 1-81.

14. Ladanyi, B. and Archambault, G. Simulation of shear behaviour of a jointed rock mass. 11th. Symp. Rock Mech.
Berkeley 1969. Ch. 7, pp. 105-125.

15. Deere, D.U., Hendron, A.J. Patton, F.D. and Cording, E.J. Design of surface and near-surface construction in rock. 8th. Symp. Rock Mech. Minnesota 1966. Ch. 11, pp. 237-302.

16. Seraphim, J.L. and Guerreiro, M. Shear strength of rock masses at three Spanish dam sites. Int. Symp. Rock Mech. Madrid 1968. II.4, pp. 147-158.

17. Barton, N.R. A low strength material for simulation of the mechanical properties of intact rock in rock mechanics models. Proc. 2nd. Cong. Int. Soc. Rock Mech. Belgrade 1970, Paper 3-15. Vol. 2.

18. Krsmanovic, D., Tufo, M. and Lanof, Z. Shear strength of rock masses and possibilities of its reproduction on models. Proc. 1st. Cong. Int. Soc. Rock Mech., Lisbon 1966, Paper 3-52.

19. Goodman, R.E. The deformability of joints. Symposium: Determination of the in situ modulus of deformation of rock. A.S.T.M. S.T.P. 477 1970, pp. 174-196.

20. Wickens, E.H. and Barton, N.R. Application of photogrammetry to the stability of excavated rock slopes. Photogrammetric Record. (Photogrammetry Society, London). No. 37, Vol. 6, April 1971.

21. De Freitas, M. Personal communication. Eng. Geol. Dept. Imperial Coll., London 1970.

22. Hoek, E. Brittle failure of rock. Rock Mechanics in Engineering Practice. Eds. Stagg and Zienkiewicz. J.Wiley and Sons. Ch. 4, 1968.

23. Barton, N.R. Estimation of in situ shear strength from back analysis of failed rock slopes. Int. Symp. Rock Mech. Nancy 1971 (Theme 2 of this symp.).

24. Rengers, N. Influence of surface roughness on the friction properties of rock planes. Proc. 2nd Cong. Int. Soc. Rock Mech. Belgrade 1970, paper 1-31. Vol. 1.

25. Cundall, P.A. Personal communication. Rock Mech. Dept. Imperial College, London 1970.

26. Broch, E. The influence of size and shape on the point load strength of rocks. University of London. M.Sc. Thesis. 1970.

27. Franklin, J.A., Broch, E. and Walton, G. Logging the mechanical character of rock. Imperial College. Rock Mech. Res. Rept. No. D 14, July 1970.

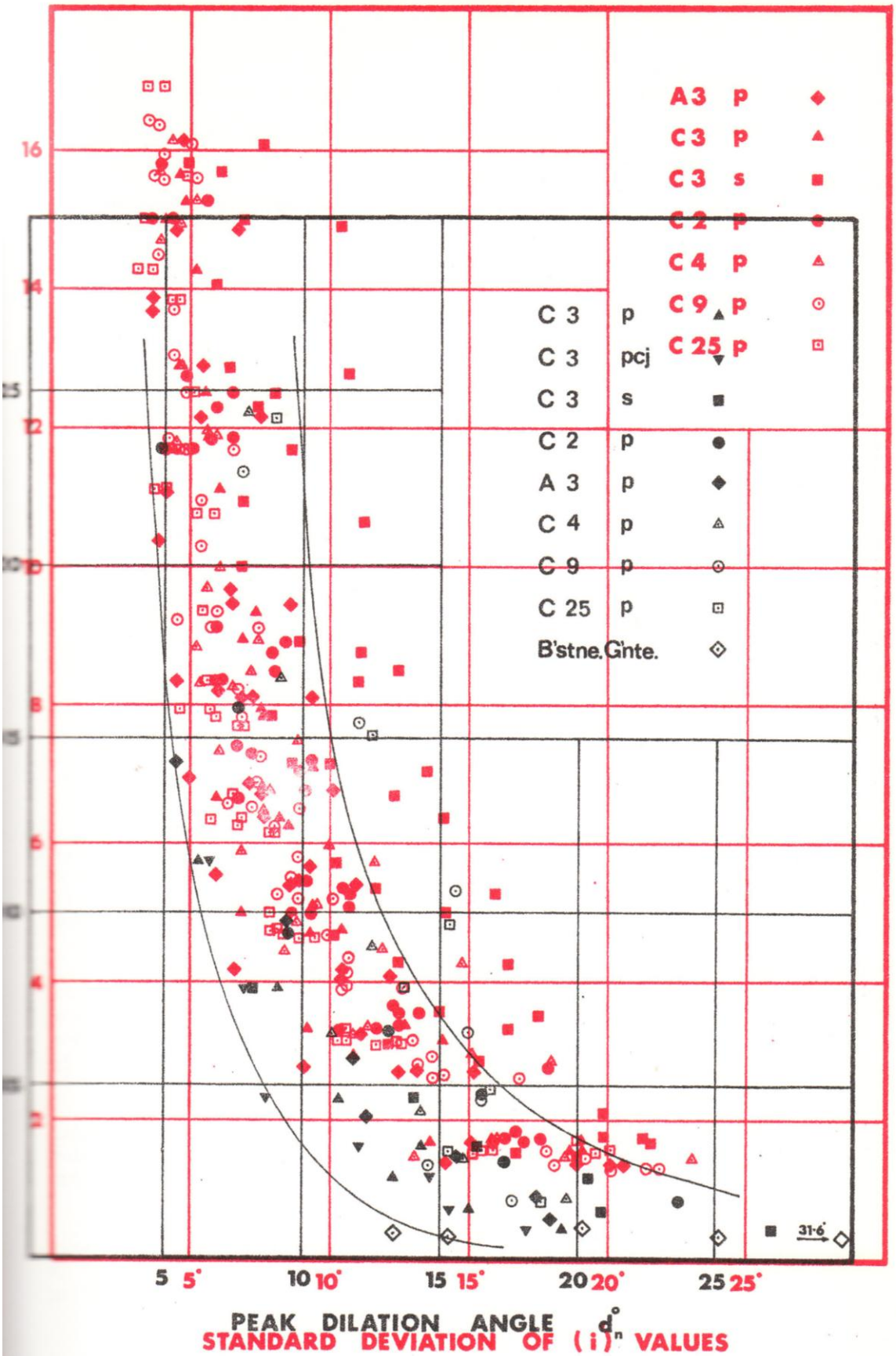

Figure 2.1.25 A statistical shearing analogy.

(See Fig. 17)

..